frontiers | Frontiers in Chemical Biology

TYPE Original Research
PUBLISHED 22 May 2024
DOI 10.3389/fchbi.2024.1398105

OPEN ACCESS

EDITED BY
Ana Maria Da Costa Ferreira,
University of São Paulo, Brazil

REVIEWED BY
Chunmao He,
South China University of Technology, China
Michal Jan Gajda,
Migamake Pte Ltd., Singapore

*CORRESPONDENCE
Sofia R. Pauleta,
sofia.pauleta@fct.unl.pt

†PRESENT ADDRESS
Cristina M. Cordas,
HyLab-Green Hydrogen Collaborative Laboratory, Central Termoelétrica de Sines, Sines, Portugal

RECEIVED 08 March 2024
ACCEPTED 02 May 2024
PUBLISHED 22 May 2024

CITATION
Mordido VH, Carepo MSP, Cordas CM, Paul N, Simon J, Moura I and Pauleta SR (2024), Effect of pH on the thermostability and redox properties of cytochrome c_{552} from *Wolinella succinogenes*.
Front. Chem. Biol 3:1398105.
doi: 10.3389/fchbi.2024.1398105

Effect of pH on the thermostability and redox properties of cytochrome c_{552} from *Wolinella succinogenes*

Vitor H. Mordido[1,2,3], Marta S. P. Carepo[3,4], Cristina M. Cordas[3†], Navendu Paul[3], Jörg Simon[5], Isabel Moura[3] and Sofia R. Pauleta[1,2*]

[1]Microbial Stress Lab, UCIBIO-Applied Molecular Biosciences Unit, Department of Chemistry, NOVA School of Science and Technology, Universidade NOVA de Lisboa, Caparica, Portugal, [2]Associate Laboratory I4HB-Institute for Health and Bioeconomy, NOVA School of Science and Technology, Universidade NOVA de Lisboa, Caparica, Portugal, [3]Associated Laboratory for Green Chemistry (LAQV), Department of Chemistry, NOVA School of Science and Technology, Universidade NOVA de Lisboa, Caparica, Portugal, [4]EPCV—Department of Life Sciences, Lusófona University, Lisbon, Portugal, [5]Microbial Energy Conversion and Biotechnology, Department of Biology, Technische Universität Darmstadt, Darmstadt, Germany

Cytochrome c_{552} from *Wolinella succinogenes* is one of the few examples of a low reduction potential class I *c*-type cytochrome with a mixture of high/low spin state populations observed in its visible spectrum. Analysis of its structural model suggests that the heme is Met/His coordinated and highly solvent-exposed. This supports the hypothesis that it is the solvent accessibility of the propionate groups that controls the reduction potential of this small *c*-type cytochrome. The visible spectra obtained at different pH values reveal the presence of a protonable group with a pK_a of 7.3, which also influences the reduction potential of this small cytochrome c_{552} ($E_m^{0'}$ of 97 ± 5 mV, pH 7.0) and can be either an H_2O/OH^- group distantly coordinating the heme iron, or one of the propionate groups. The thermostability of cytochrome c_{552} was studied by circular dichroism and differential scanning calorimetry, indicating a highly stable protein at pH 5–7 (90°C to 77°C).

KEYWORDS

cytochrome *c*, *Wolinella succinogenes*, pH effect, thermostability, circular dichroism, differential scanning calorimetry, cyclic voltammetry

1 Introduction

Denitrifying organisms reduce nitrate to nitrogen in four steps, each catalyzed by a metalloenzyme: nitrate reductase (Sparacino-Watkins et al., 2014), nitrite reductase (Besson et al., 2022), nitric oxide reductase (Shiro, 2012), and nitrous oxide reductase (Pauleta et al., 2013). This enzyme catalyzes the final step of this pathway, denitrification, which is the reduction of nitrous oxide to dinitrogen, according to Eq. 1 (Pauleta et al., 2019).

$$N_2O + 2\,e^- + 2\,H^+ \rightarrow N_2 + H_2O, E^{o\prime} = 1.35\,V, pH\,7.0 \quad (1)$$

Nitrous oxide reductase is a multiple copper enzyme with two copper centers: CuA a binuclear electron transfer center, and the catalytic site CuZ, which contains four copper atoms. The two electrons required for the reduction are delivered to the CuA center by small redox proteins, T1 copper proteins or *c*-type cytochromes (Dell'Acqua et al., 2008; Fujita et al., 2012).

These small *c*-type cytochromes belong to the class I because they have about 120 residues, with the heme-binding motif, -CXXCH-, near the N-terminus, and the sixth ligand, a methionine residue, 40 residues toward the C-terminus. Thus, the heme is covalently bound to the polypeptide chain by two thioether bonds and it is Met/His hexacoordinated, being usually in a low-spin configuration with a reduction potential of about +250 mV *versus* NHE at pH 7.0 (Senn and Wüthrich, 1985; Ferri et al., 1996). Structurally these cytochromes have three to six α-helices, with the heme being shielded from the solvent (Bertini et al., 2006).

The bacterium *W. succinogenes* can reduce nitrate to ammonia in a respiratory process, but is also capable of reducing nitric oxide and nitrous oxide gases (Payne et al., 1982; Kern and Simon, 2009). *W. succinogenes* cytochrome *c* nitrous oxide reductase has been isolated and a small cytochrome *c* of 81 residues has been proposed as its possible physiological electron donor (Teraguchi and Hollocher, 1989; Zhang and Hollocher, 1993). In addition, this small cytochrome *c* is also predicted to mediate electron transport between the Rieske cytochrome *bc* complex and the cytochrome cbb_3 oxidase and was first isolated by our group in 1988 (Moura et al., 1988; Baar et al., 2003; Kern et al., 2010). Visible spectroscopy, as well as NMR studies suggested the presence of an equilibrium between two ligand arrangements around the heme (a high spin form coexisting with a low spin form of the heme, with methionine coordination) and a reduction potential lower than usual, +105 mV, pH 7.6 (Moura et al., 1988).

Another small *c*-type cytochrome has been isolated in our group from a denitrifying marine bacterium, *Marinobacter nauticus*, cytochrome c_{552}. Although, also smaller than the usual class I cytochromes, its reduction potential is higher, +250 mV at pH 7.6 (Saraiva et al., 1994). This small *c*-type cytochrome is always a dimer in solution and no high-spin form has been observed. The structural similarities and the different spectroscopic properties of these two rather small *c*-type cytochromes are discussed here.

In this paper we describe the heterologous production of cytochrome c_{552} from *W. succinogenes*. The spectroscopic characterization of this small *c*-type cytochrome is further investigated by various techniques, correlated with our previous results, and interpreted in the light of the structural model reported here. The thermostability of this protein has been studied by differential scanning calorimetry and circular dichroism. The system for its heterologous production will allow us to proceed with electron transfer studies with cytochrome *c* nitrous oxidase reductase.

2 Materials and Methods

2.1 Chemicals

Unless otherwise stated, all reagents were of analytical or higher grade and were purchased from Sigma-Aldrich, Merck and Fluka. Solutions were prepared in bi-distilled water or Milli-Q water where indicated.

2.2 Bioinformatic analysis

The DNA sequence of cytochrome c_{552} from *W. succinogenes* (WS0700) was obtained from the GenBank (http://www.ncbi.nlm.nih.gov/genbank) to design the primers. All the analyzed protein sequences were obtained from the Protein database at NCBI (http://www.ncbi.nlm.nih.gov/protein). Multi-sequence alignments were performed using the Clustal Omega (Sievers et al., 2011). Prediction of a signal peptide was performed using SignalP—6.0 (Teufel et al., 2022). A structural model of the globular domain of *Ws* cytochrome c_{552} was generated using AlphaFold colab (Jumper et al., 2021), which has a per-residue confidence greater than 90, indicating a high degree of confidence in the coordinates of the polypeptide chain (Supplementary Figure S2, in the Supplementary Material). The heme group was manually added, according to the following procedure. The coordinates of the heme group were those of *M. nauticus* cytochrome c_{552} after superposition of the model structure with this structure (global RMDS of 1.8 Å). The superposition of the two structures (Supplementary Figure S9, in the Supplementary Material) showed that the atoms coordinating the heme iron (Nε2 of His14 and Sδ of Met58), as well as the sulfur atoms of the two cysteine residues (Cys10 and Cys13) forming the thioether bond with the heme, are superimposed. In this way, the thioether bond was formed with the vinyl groups at the β-pyrrole positions two and four of the heme, and this model structure was used to generate the figures shown in the manuscript. In this structure, the distance between the coordinating atoms and the heme iron was similar to other structures (2.0 Å and 2.2 Å for the N-Fe and S-Fe, respectively), and the angles of the thioether bond were 100° and 109° (which compares well with 105° and 108° in the *M. nauticus* cytochrome c_{552} structure).

2.3 Heterologous production of *Wolinella succinogenes* cytochrome c_{552}

The gene encoding *W. succinogenes* cytochrome c_{552} (WS0700), hereafter referred to as *Ws* cytochrome c_{552}, was amplified by PCR using a set of primers (forward: CATGCCATGGCTGATGGTGCA ACCCTCTA, and reverse: CTGGCTCGAGTTACTTGAGCGTGG AGATGTAT) with a NcoI and a XhoI restriction site at the 5′ and 3′-ends, respectively. The amplified fragment encoding the mature cytochrome c_{552}, excluding its signal peptide (residue 1 to 17, Supplementary Figure S1, in the Supplementary Material), was cloned into a pET22b (+) plasmid, hereafter designated as pET22-*Ws*cytc. The plasmid confers ampicillin resistance and adds an N-terminal signal peptide (*pelB*) to direct the protein to the periplasm. This cloning strategy introduced an additional Met residue, at the N-terminus after cleavage of the signal peptide, giving the mature protein 82 residues.

Escherichia coli DH5α (Invitrogen) was used for plasmid propagation. *Ws* cytochrome c_{552} was produced in *E. coli* C41 (DE3) (Merck) co-transformed with pET22-*Wscytc* and pEC86 (which harbors the *ccm* genes for production of the machinery for *c*-type heme biosynthesis and maturation (Arslan et al., 1998), and confers chloramphenicol resistance). Four to five colonies of the co-transformed *E. coli* C41 (DE3) were used to inoculate 50 mL of Luria-Bertani (LB) medium (10 g tryptone, 10 g NaCl and 5 g yeast extract, per liter) supplemented with 100 μg/mL ampicillin and 30 μg/mL chloramphenicol and grown overnight at 37°C, 210 rpm. Fresh 2xYT medium (16 g tryptone, 5 g NaCl and 10 g yeast extract, per liter), supplemented with the same antibiotics, was

inoculated with 1% of the pre-inoculum. Cultures were incubated under orbital shaking at 37°C, 210 rpm until an $OD_{600\ nm}$ of 0.6 was reached. At this point, gene expression was induced with 0.25 mM IPTG for 18 h at 30°C, 120 rpm. Cells were harvested at 8000 × *g*, six°C, 15 min, and resuspended in 50 mM Tris-HCl, pH 7.6 containing protease inhibitors (cOmplete™, Mini, EDTA-free, Protease Inhibitor Cocktail Tablets, Roche).

2.4 Purification of heterologous *Wolinella succinogenes* cytochrome c_{552}

The periplasmic fraction was obtained by four freeze-thaw cycles and separated from spheroplasts and cell debris by centrifugation at 39,000 *g*, 6°C, 45 min. Purification was performed in a single chromatographic step, using a cationic exchange chromatography. The periplasmic fraction was diluted 10× with cold milli-Q water and loaded onto a CM52 (Cytiva) cation-exchange chromatographic column (12.5 cm x 3 cm ∅, 90 mL), equilibrated with 5 mM sodium phosphate buffer, pH 7. Protein not adsorbed on the matrix was eluted with 5 mM sodium phosphate buffer, pH 7, and then a linear gradient between 0 and 500 mM NaCl was applied. The *Ws* cytochrome c_{552} eluted with 125 mM NaCl, and the fractions with $A_{408.5nm}/A_{280nm}$ above 4.7 were considered pure, combined, and concentrated over a 3 kDa MWCO membrane using a Vivaspin 15 centrifugal device (Sartorius). The final *Ws* cytochrome c_{552} fraction was buffer exchanged to 5 mM Na-phosphate pH 7.0 using a desalting PD-10 column (Cytiva). A 15% SDS-PAGE and 10% PAGE stained for protein (Coomassie blue) and heme content (Goodhew et al., 1986) was also used throughout the purification to verify the protein purity. *Ws* cytochrome c_{552} was stored in small aliquots at—80°C until further use. Protein and heme content were estimated in the same solution for which the CD spectra in the far-UV region was obtained: protein was quantified using the extinction coefficient at 205 nm determined for CD (see below) and heme content by the pyridine hemochrome assay (Berry and Trumpower, 1987). Molecular mass was determined by LC-ESI-MS (Bruker) using a µPACTM analytical column from PharmaFluidics. The *Ws* cytochrome c_{552} from the same purification batch was used for all the spectroscopic and biophysical analyses: the protein was desalted in the buffer with different pH values (see below) and then used in the different experiments.

2.5 Spectroscopic characterization

The UV-visible spectra were recorded on a Shimadzu UV-1800 spectrophotometer, connected to a computer, using a 1 cm path quartz cuvette. The concentration of the protein was estimated using the reported molar extinction coefficient of 80.1 $mM^{-1}cm^{-1}$ at pH 7.6, 100 mM Na-phosphate buffer (Moura et al., 1988). *Ws* cytochrome c_{552} in the reduced state was obtained by reduction with a solution of sodium dithionite, with a final concentration of 5 mM.

Circular dichroism spectra were acquired in an Applied Photophysics ChirascanTM qCD spectrometer (Leatherhead, Surrey, United Kingdom). Far-UV (190–260 nm) spectra were acquired in a sample of 8.5–10.6 µM *W* cytochrome c_{552}, in 5 mM Na-phosphate buffer, pH 5.0, 6.0, 7.0, 8.0, and 9.0, using a 1 mm path length cuvette with a total volume of 300 µL. In the visible region (260–800 nm) the spectra were recorded for a 35 µM *W* cytochrome c_{552} sample, in 5 mM Na-phosphate buffer, pH 7.0, using a 10 mm path length cuvette with a total volume of 2.3 mL. The concentration of the samples was determined using the absorbance at 205 nm and the extinction coefficient of 290,700 $mM^{-1}\,cm^{-1}$, based on the amino acid content (Anthis and Clore, 2013), or the absorbance at 408 nm and the extinction coefficient mentioned before. CD data were reported in mean residue ellipticity ($[\theta]_{MRE}$) as a function of wavelength. The $[\theta]_{MRE}$ is the CD raw data (in deg) corrected for the *Ws* cytochrome c_{552} concentration of the solution using Eq. 1:

$$[\theta]_{MRE} = \frac{\theta(\deg) \times MRW}{10 \times L \times C} \quad (1)$$

where MRW (mean residue weight) is the molecular mass of *Ws* cytochrome c_{552} divided by the number of peptide bonds (81), C is the concentration of the protein in the sample in $g \bullet mL^{-1}$, and L is the pathlength of the cell in cm.

The CD spectra between 190 and 260 nm are an average of three spectral acquisitions at 25°C, with a bandwidth and step-size of 1 nm, and acquired with a time per point of 3 s. The far-UV data analysis to determine the secondary structure content was performed using the BeStSel server (https://bestsel.elte.hu/) (Micsonai et al., 2021; Micsonai et al., 2022). The CD spectra between 260 and 800 nm are an average of three spectral acquisitions at 25°C, with a bandwidth and step-size of 1 nm, and acquired with a time per point of 3 s. The temperature-dependent CD spectra were acquired between 10°C and 94°C, with a stepped ramp mode of 1 s per point, an increase of 2°C for each measurement, and a stabilization period of 1 min between each point.

The unfolding process was analyzed using the Gibbs–Helmholtz method - to fit the change in ellipticity at a single wavelength as a function of temperature, considering a two-state transition from a folded native state to an unfolded state, and assuming that the heat capacity of the folded and the unfolded states are equal, ΔCp = 0 (Greenfield, 2004). For the Gibbs–Helmholtz method, the experimental data were fitted using Eqs. 2–5 and using the SOLVER add-in program of Microsoft Excel. The molar ellipticity at any given temperature (T), $(\theta)_T$, is given by Eq. 2:

$$[\Theta]_T = \alpha \times ([\Theta]_F - [\Theta]_U) + [\Theta]_U,, \quad (2)$$

in which the fraction folded at any given temperature, α, is given by Eq. 3:

$$\alpha = \frac{K}{1+K} \quad (3)$$

and the folding constant, K, at any given temperature is given by Eq. 4:

$$K = \exp\left(\frac{-\Delta G}{R \times T}\right) \quad (4)$$

and ΔG is given by Eq. 5:

$$\Delta G = \Delta H \times \left(1 - \frac{T}{T_M}\right) \quad (5)$$

in which T_M is the temperature at which the fraction folded, α, is 0.5.

```
Ws Cyt c552 -----ADGATLYKKCVACHGVKAEKPALGKSEVIAGWD-KAKLVEEL---KAYKAGTLNR   51
Mn Cyt c552 -AGDIEAGKAKAAVCAACHGQNGISQV-PIYPNLAGQK-EQYLVAAL---KAYKAGQRQG   54
Nv Cyt c553 -----ADGAALYKSCIGCHGADGSKAAMGSAKPVKGQG-AEELYKKM---KGYADGSYGG   51
                  * :    * .*** .. . .      : *      *   :   *.*  *
Pd Cyt c550 QDGDAAKGEKEFNKCKACHMIQAPDGTD----IIKGGKTGPNLYGVVGRKIASEEGFKYG   56
                  *      * .**  .. . .      : *      *   :    .   *

Ws Cyt c552 NGMGAM-MKGQMASFSDADIEA--------------------------------VSEYIS   78
Mn Cyt c552 G-QAPV-MQGQATALSDADIAN--------------------------------LAAYYA   80
Nv Cyt c553 E-RKAM-MTNAVKKYSDEELKA--------------------------------LADYMS   77
                 : * .     ** ::                                  :: * :
Pd Cyt c550 EGILEVAEKNPDLTWTEADLIEYVTDPKPWLVKMTDDKGAKTKMTFKMGKNQADVVAFLA   116
                 :   .     :: ::                                  :  : :

Ws Cyt c552 TLK----------   81
Mn Cyt c552 SLPADGQG-----   88
Nv Cyt c553 KL-----------   79
            .*
Pd Cyt c550 QNSPDAGGDGEAA   129
```

FIGURE 1
Primary sequence alignment of the mature cytochrome c_{552} from *Wolinella succinogenes* with the mature sequence of other small cytochromes *c*, with similar function and structure. The heme-binding motif and the axial ligands are shown in bold. Asterisks, colons, or stops below the sequence indicate identity, high conservation, or conservation, respectively of the amino acids between the first three or all the sequences. Legend: *Ws* Cytc$_{552}$ (*Wolinella succinogenes* cytochrome c_{552}, Q7MS72), *Nv* Cytc$_{553}$ (*Nitratidesulfovibrio vulgaris* Hildenborough cytochrome c_{553}, P04032), *Mn* Cytc$_{552}$ (*Marinobacter nauticus* cytochrome c_{552}, P82903) and *Pd* Cytc$_{550}$ (*Paracoccus denitrificans* cytochrome c_{550}, P00096).

2.6 Differential scanning calorimetry

For the differential scanning calorimetry (DSC) experiments, the NanoDSC instrument (TA Instruments) was loaded with degassed buffers (baselines and reference cell) and protein solution (83–93 μM *Ws* cytochrome c_{552} in the sample cell). Each protein sample was passed through a desalting PD-10 column (Cytiva) equilibrated in the appropriate buffer (5 mM Na-phosphate buffer at pH 5.0, 6.0, 7.0, 8.0, and 9.0) and then diluted to the desired concentration in the same buffer. The temperature was raised from 10 to 120°C at a scan rate of 1°C/min, and 6 bar. The thermograms were analyzed with TA instruments NanoAnalyze software using a non-two-state model to fit the data and obtain the melting temperature (T_M), the calorimetric (ΔH) and van't Hoff (ΔH_v) enthalpies. The corresponding baseline was subtracted from each sample scan.

2.7 Determination of the reduction potential

Cyclic voltammetry assays were performed in a single compartment cell with a three-electrode configuration. A cysteamine-modified gold disk (ϕ = 2 mm) was used as the working electrode and a platinum foil and a saturated calomel electrode (SCE) were used as the secondary and reference electrodes, respectively. The gold electrode was modified by immersion in a 2 mM cysteamine solution for 30 min at room temperature (RT), followed by washing by immersion in deionized water. The protein (5 μL of approx. 550 μM) was then placed on the modified gold electrode and a cellulose membrane (3.5 kDa cut-off) was then applied for protein entrapment and studied in a thin-layer regime. The used electrolyte was a mixed 20 mM phosphate/acetate buffer/0.1 M NaCl, at different pH values or only 20 mM phosphate/0.1 M NaCl, pH 7. Assays were performed at RT in a strictly anaerobic environment inside an anaerobic chamber (c_{O2}<0.1 ppm). Different potential windows and scan rates were tried. All the potentials were converted and presented in the normal hydrogen electrode (NHE) reference scale. Controls were obtained using the same procedure and conditions without the presence of the protein.

3 Results

3.1 Primary sequence analysis and structural model

Analysis of the primary sequence of the mature cytochrome c_{552} from *W. succinogenes* (81 residues) reveals the presence of an N-terminal heme-binding motif and a conserved methionine residue, about 40 residues away toward the C-terminus, as a distal axial ligand of the heme iron. These features suggest that this *c*-type cytochrome belongs to class I, subdivision b (Pettigrew and Moore, 1987).

In Figure 1 is shown the sequence alignment of the primary sequence of the mature cytochrome c_{552} from *W. succinogenes* with two *c*-type cytochromes that are electron donors of nitrous oxide reductase from *M. nauticus* (Dell'Acqua et al., 2008; Dell'acqua et al., 2011), cytochrome c_{552}, and from *Paracoccus denitrificans*, cytochrome c_{550} (Pearson et al., 2003; Dell'acqua et al., 2011),

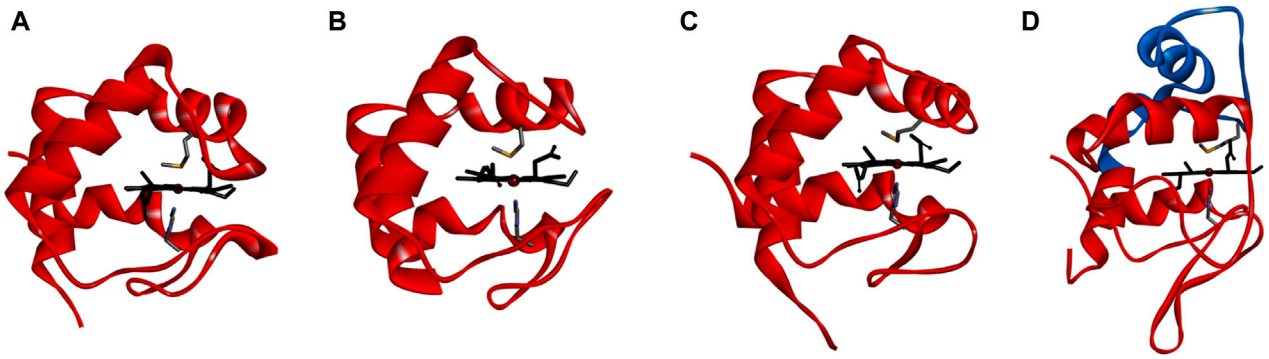

FIGURE 2
Structure of small *c*-type cytochromes. Comparison of the structural model of cytochrome c_{552} from *Wolinella succinogenes* obtained using the Alphafold colab Panel **(A)**, with the structures of *Nitratidesulfovibrio vulgaris* Hildenborough cytochrome c_{553} (PDB ID 1DVH, average structure) Panel **(B)**, *Marinobacter nauticus* cytochrome c_{552} (PDB ID 1CNO:A) Panel **(C)**, showing only monomer A) and *P. denitrificans* cytochrome c_{550} (PDB ID 1COT) Panel **(D)**. The heme group and axial ligands are shown as sticks colored in black or by atom (carbon in grey, nitrogen in blue and sulfur in yellow). The additional helices in *P. denitrificans* cytochrome c_{550} are colored in blue. Figure was prepared in BIOVIA Discovery Visualizer Studio using the coordinates indicated above.

and the cytochrome c_{553} from *Nitratidesulfovibrio vulgaris* Hildenborough (formerly known as *Desulfovibrio vulgaris* Hildenborough), which has a low reduction potential (*vide infra*) compared to other class I *c*-type cytochromes (Pettigrew and Moore, 1987). The sequence identity between these cytochromes is relatively low (34%, 35%, and 23% with the *c*-type cytochromes from *M. nauticus*, *Nitratidesulfovibrio vulgaris* Hildenborough, and *P. denitrificans*, respectively), but they all share the conserved heme-binding motif and the position of the axial methionine toward the C-terminus. The alignment shows that cytochrome c_{550} from *P. denitrificans* is longer, with an inserted region between residue 78 and 110 containing the coordinating methionine. The high sequence homology at the two extremities could indicate a transposition.

The structural model of this protein was obtained using AlphaFold colab (Supplementary Figure S2, in the Supplementary Material), and the heme group was added as described in Materials and Methods. This structure shows that it is composed of 4 α-helices and that the heme group is more solvent exposed than in the case of *P. denitrificans* cytochrome c_{550} (Figure 2D; Supplementary Figure S9 in the Supplementary Material), since the loops covering the heme and an extra helix are missing (Figure 2D, RMSd of 3.3 Å and TM-score of 0.55; Supplementary Table S1, in the Supplementary Material), as expected from the analysis of the sequence alignment (Figure 1). Comparison of its structure with that of the small *c*-type cytochrome from *M. nauticus* and *N. vulgaris* Hildenborough (RMSd of 1.8 and 1.0 Å, and TM-score of 0.86 and 0.89, respectively, Supplementary Table S1, in the Supplementary Material), shows that their structure and heme accessibility are similar (Figure 2; Supplementary Figure S9, in the Supplementary Material), although in the case of *M. nauticus* cytochrome c_{552} the heme is less exposed to the solvent because it is a dimer (Supplementary Figure S11, in the Supplementary Material). The superposition of the four structures highlights that the long loop in *P. denitrificans* cytochrome c_{550} is a α-helix in the other structures, and that there are also two short β-sheets that are absent in the small cytochromes. An important feature is that, although the structures have differences, the heme coordinating residues are well aligned in the structure (Supplementary Figures S9 and S10; Supplementary Table S2 in the Supplementary Material), although this is not shown in the sequence alignment (Figure 1). This structural difference supports the classification of *Ws* cytochrome c_{552} and the other two small cytochromes as belonging to subdivision Ib, whereas *P. denitrificans* cytochrome c_{550} belongs to subdivision Ia (Pettigrew and Moore, 1987).

3.2 Heterologous production of *Wolinella succcinogenes* cytochrome c_{552}

The DNA fragment amplified by PCR and inserted into the pET22b expression vector encoded only the globular region of *Ws* cytochrome c_{552}, starting at A18, and due to cloning an additional Met residue was added at the N-terminus (Supplementary Figure S1, in the Supplementary Material). This recombinant protein has 82 residues, after removal of the PelB signal peptide, and an expected molecular mass of 9342.7 Da (8728.2 Da plus 614.5 Da, which is the sum of the molecular mass of the polypeptide chain and one heme group).

The *Ws* cytochrome c_{552} was isolated from the periplasm of *E. coli* in a single chromatographic step, consisting of a cationic exchange chromatography, since the pI of this protein is 8.6. The cytochrome *c* was considered pure according to its SDS-PAGE and PAGE profile (Supplementary Figure S3, in the Supplementary Material) with a single band, and this fraction had a purity ratio [A_{552nm}–A_{570nm} (reduced form)/A_{280nm} (oxidized form)] of 1.20. This procedure has an average yield of 46 mg of pure *Ws* cytochrome c_{552} per liter of growth medium. The heme/protein ratio of the purified cytochrome *c*, as determined by heme and protein concentration (see Materials and Methods), was 0.89 ± 0.02, confirming the presence of 1 *c*-type heme bound to the polypeptide chain, as expected. The molecular mass of the purified *Ws* cytochrome c_{552} was determined by LC-ESI-MS to be 9342.53 ±

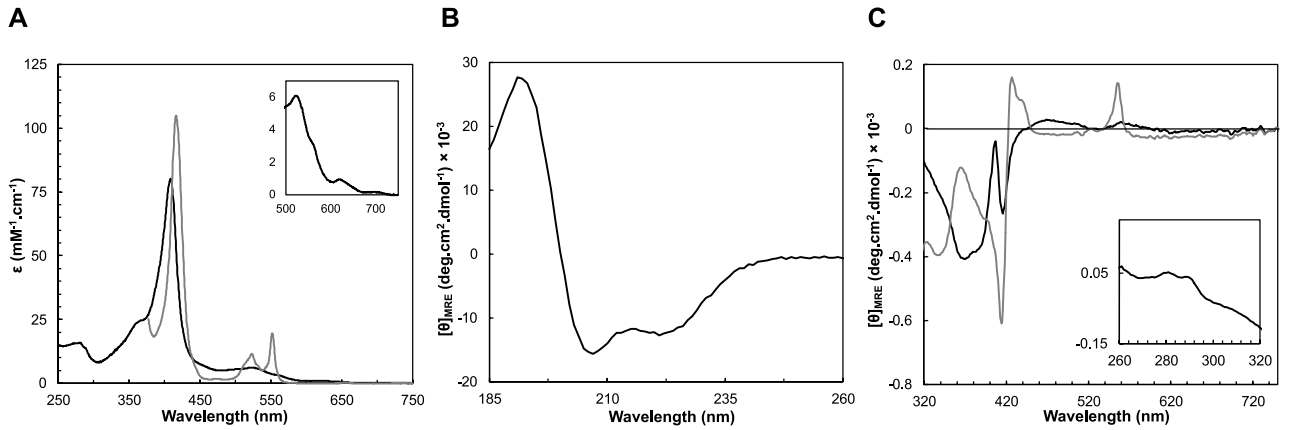

FIGURE 3
Spectroscopic features of *Ws* cytochrome c_{552} in the as-isolated (black line) and reduced state (grey line) at pH 7.0. **(A)** UV-visible spectra acquired in the as-isolated and reduced state. Inset shows the Q-band region. Circular dichroism spectra in the far-UV **(B)** and visible **(C)** regions acquired in the two oxidation states, at 25°C. The inset in panel C shows the near-UV region of the CD spectrum of the oxidized state.

0.04 Da, confirming the correct processing of the signal peptide and the presence of the *c*-type heme.

3.3 Spectroscopic characterization

The UV-visible spectrum of the heterologous cytochrome *c* shows similar spectral features to the same protein isolated from *W. succinogenes* (Moura et al., 1988) (Figure 3A), namely, the Soret band at 409 nm, and absorption bands with maxima at 620 nm and 695 nm, indicating the presence of a high-spin state, and a methionyl residue (Met59, numbering according to the mature sequence), respectively. The extinction coefficient estimated based on the heme content is identical to that reported, 80.1 $mM^{-1}cm^{-1}$ at pH 7.6 (Moura et al., 1988).

After reduction, the Soret band shifts to 417 nm, with the appearance of the β and α bands at 523 nm and 552 nm, respectively (Figure 3A). The maximum absorption of the α-band at 552 nm, designates this cytochrome as cytochrome c_{552}, as has been for others (Hon-nami and Oshima, 1977; Saraiva et al., 1994; Samyn et al., 1998).

As previously observed, the high-spin state decreases with increasing pH, as the ratio A_{621nm}/A_{695nm} decreases (from pH 5.0 to pH 7.0 the ratio is around 6.0, decreasing to 4.7 and 4.5 at pH 8.0 and 9.0, respectively) (Table 1), indicating a p*K*a around 7.5 (Figure 5B), as previously reported (inflection point at pH 7.3 for the absorbance at 620 nm) (Moura et al., 1988).

The folding state of a protein and its secondary structure content can be determined by analyzing its circular dichroism spectra in the far-UV region (190–260 nm). The CD spectrum of the as-isolated *Ws* cytochrome c_{552} shows a positive peak at 192 nm, and two negative peaks at 208 and 222 nm, with a ratio $\theta_{222nm}/\theta_{208nm}$ of 0.8. These features indicate the presence of a folded protein composed mainly of α-helix (Figure 3B). This spectrum is similar to that of cytochrome c_{552} from *Hydrogenobacter thermophilus* and cytochrome c_{553} from *N. vulgaris* Hildenborough, cytochromes *c* composed mainly of α-helix (Wittung-Stafshede, 1999; Oikawa et al., 2005). The secondary structure content was estimated by analyzing the far-UV spectrum at 25°C, pH 7.0 using the BeStSel algorithm (Micsonai et al., 2021; Micsonai et al., 2022) and indicates the presence of 27% α-helices, with 10% of β-sheets (Table 1). These values are in agreement with the analysis of the coordinates of the structural model of this protein, which predicts a protein mainly α-helix with a small percentage of structure as β-sheets (40% α-helices, with 7% of β-sheets).

TABLE 1 Spectral features and thermostability parameters of *Ws* cytochrome c_{552} at different pH values.

	pH 5	pH 6	pH 7	pH 8	pH 9
A_{621nm}/A_{695nm}	5.9	5.6	5.3	4.7	4.5
T_M (°C) (CD)	>90	>85	>80	72.3 ± 0.2	72.5 ± 0.1
T_M (°C) (DSC)	90 ± 0.02	83 ± 0.03	77 ± 0.02	72± 0.02	70 ± 0.01
ΔH_{cal} (kJ/mol)	73	101	75	87	98
ΔH_{vH} (kJ/mol)	486± 3	337± 2	441± 3	382± 2	322± 1
$\Delta H_{cal}/\Delta H_{vH}$	0.2	0.3	0.2	0.2	0.3
$\theta_{222nm}/\theta_{208nm}$	0.77	0.77	0.81	0.78	0.78
α-helix	28%	27%	27%	32%	26%
β-sheet	12%	12%	10%	9%	12%

The near-UV and visible CD spectra of the oxidized *Ws* cytochrome c_{552} were collected in a pH range of 5–9 (Supplementary Figure S6, in the Supplementary Material). In the near-UV region, the presence of two positive bands at 282 nm and 290 nm is observed, which can be attributed to the single tryptophan residue present in the sequence, W33, which is located near the heme propionates in the predicted structure (Supplementary Figure S12, in the Supplementary Material). These bands do not change over the pH range studied. The visible region of the CD spectrum of the oxidized *Ws* cytochrome c_{552} at pH 7 has a broad negative peak between 320 nm and 400 nm with a maximum at 370 nm (Figure 3C), which has also been observed in other *c*-type cytochromes (Vinogradov and Zand, 1968). A negative well-defined S-shaped band is observed with a negative minimum at 407 nm and a negative maximum at 416 nm corresponding to the

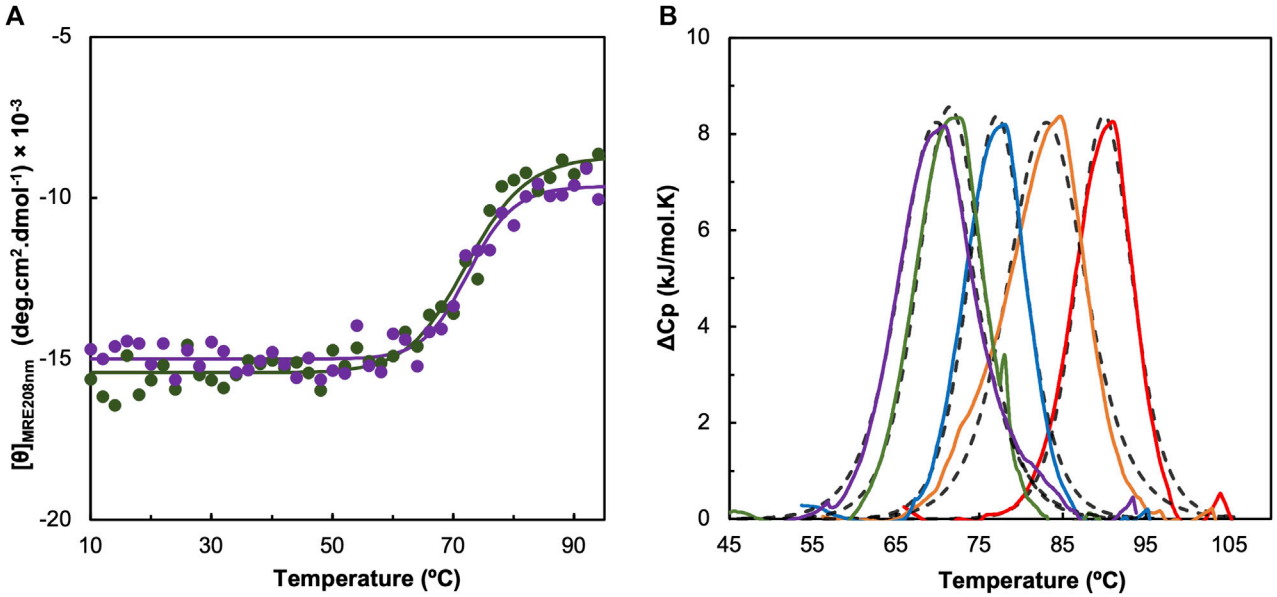

FIGURE 4
Effect of pH in the thermostability of *Ws* cytochrome c_{552} studied by circular dichroism **(A)** and differential scanning calorimetry **(B)**. Panel A shows the molar ellipticity at 208 nm obtained at different temperature for pH 8.0 (green) and pH 9.0 (purple). The experimental data were fitted using the equations for a two-state transition model (solid line). Panel B shows the thermogram of *Ws* cytochrome c_{552} obtained by DSC at pH 5.0 (red line), 6.0 (orange line), 7.0 (blue line), 8.0 (green line) and 9.0 (purple line), each fitted to a one-peak transition model for each case (dashed black line).

Soret Cotton effect. This Cotton effect on the Soret band of CD spectra has usually been associated with transitions of the heme with nearby aromatic side chains (Hsu and Woody, 1971; Pielak et al., 1986) and is a fingerprint of heme integrity. The visible CD spectra do not change significantly with the pH (Supplementary Figure S6, in the Supplementary Material, suggesting that the tertiary structure of the protein, and in particular the heme pocked is not being affected by changes in the pH. The fact that the Soret band is negative can also be explained by the parallel propionate groups on the porphyrin ring (Nagai et al., 2015), which again remains unchanged with pH for *Ws* cytochrome c_{552}. Upon reduction, the broad band with a maximum at 370 nm becomes a negative minimum and the Soret CD spectrum shows a well-defined sharp band with an inflection point at 422 nm, and a negative peak at c. a. 417 nm, followed by a positive peak at 433 with a shoulder at 440 nm. There is also a positive peak at 556 nm, which corresponds to the peak of the α-band. The changes observed in the visible CD spectra between the oxidized and the reduced forms indicate that the heme environment changes upon reduction. This has also been observed for other *c*-type cytochromes (Vinogradov and Zand, 1968).

3.4 Effect of pH in the thermostability

The influence of pH on the thermostability of cytochrome c_{552} was studied by CD in the far-UV region and differential scanning calorimetry (DSC) (Figure 4), which provide complementary information on the unfolding equilibrium. The CD in the far-UV region monitors the change in secondary structure content, while DSC provides information about the overall unfolding process of the protein.

The far-UV CD spectra at different pH values, acquired at 25°C have similar spectral features to those described at pH 7.0: the peaks have the same maxima and minima (no shifts were observed) (Supplementary Figure S5, in the Supplementary Material). However, the ratio of $\boldsymbol{\theta_{222nm}/\theta_{208nm}}$ decreases at higher and lower pH values, indicating that there is a change in the alpha-helix content. Analysis of these spectra using the BeStSel algorithm confirms this small change in the secondary structure content (Table 1), with a decrease in alpha-helix content at pH 5.0, 6.0 and 9.0.

The thermostability studied by CD in the far-UV region shows that this protein is highly stable up to 60°C, independent of pH (Figure 4A). The T_M could only be estimated for pH 8.0 and 9.0, because at lower pH values no stabilization of the ellipticity up to 94°C was observed. At these two pH values, the estimated T_M was 73°C, but the process is not reversible (Supplementary Figure S7, in the Supplementary Material).

The thermogram obtained by DSC shows a single sharp endothermic peak, which was fitted to a one-peak transition model, from which a transition temperature, and a van't Hoff enthalpy of unfolding, ΔH_{vH}, was estimated (Table 1). The shape of the thermogram shows that there is a sharp decrease, indicating that the protein aggregates in solution (Supplementary Figure S4, in the Supplementary Material), which is confirmed by the small ratio $\Delta H_{cal}/\Delta H_{vH}$ (Table 1). This phenomenon occurs for all the pH values studied. The unfolding temperature shows the same trend as that observed for CD, indicating that this cytochrome c_{552} is more stable at lower pH values.

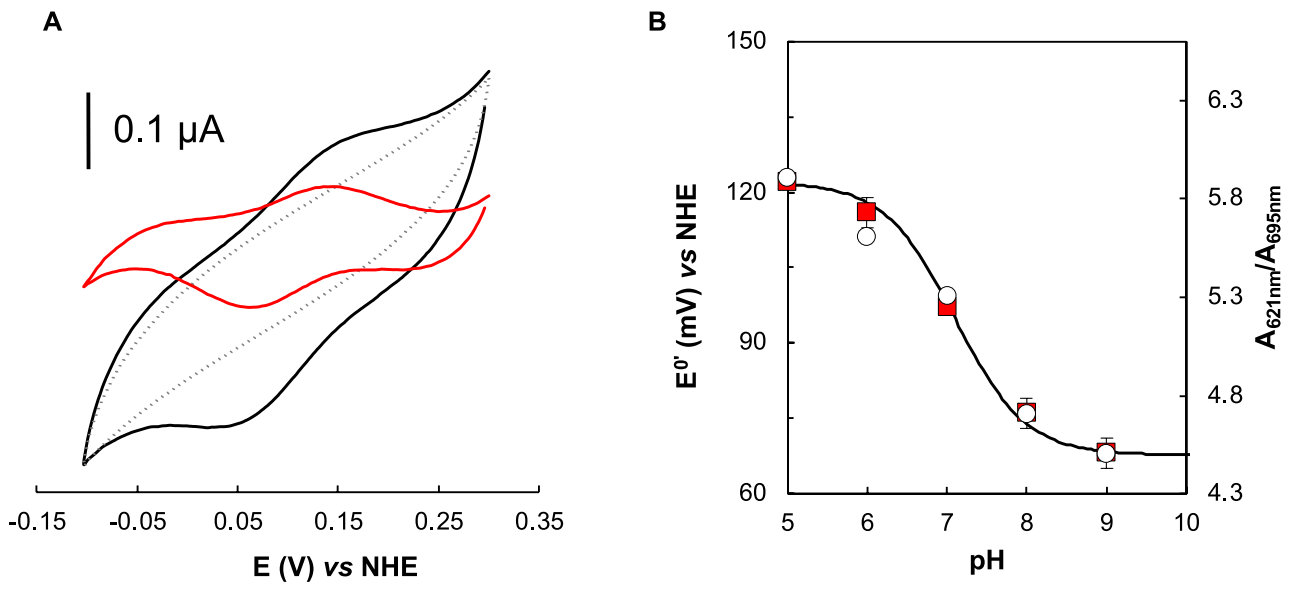

FIGURE 5
Effect of pH in the reduction potential of *Ws* cytochrome c_{552} studied by cyclic voltammetry. **(A)** Representative voltammogram of the *Ws* cytochrome c_{552} (with baseline subtraction, black line, and after control subtraction, red line), and the corresponding control in the absence of the protein (grey line) attained on cysteamine modified gold electrode, at scan rate of 50 mV s^{-1}, 20 mM phosphate buffer/0.1 M NaCl, pH 7.0, RT, in strict anaerobic environment (anerobic chamber, O_2 < 0.1 ppm). **(B)** Formal reduction potential dependence on the pH (red squares). Experimental conditions: average of all replicates (min. 3) and corresponding standard deviation. The data were fitted considering a single protonable group with a pK_{ox} and a pK_{red}, of 6.9 and 7.3, respectively. In the secondary yy axis is represented the A_{621nm}/A_{695nm}, that shows the same pH profile.

TABLE 2 Reduction potential and length of mature small class I *c*-type cytochromes from different organisms. The pKa presented was observed for the reduction potential.

Protein	Length (aa)	E^0 (mV)	pKa	Ref.
W. succinogenes cytochrome c_{552}	81	+97, pH 7.0	6.9/7.3	This work
M. nauticus cytochrome c_{552}	88	+250, pH 7.6	7.3/9.0	Saraiva et al. (1994)
N. vulgaris cytochrome c_{553}	79	+65 ± 5, pH 7.0	10.9	Verhagen et al. (1994)
P. denitrificans cytochrome c_{550}	135	+253 ± 5, N/A	-	Gray et al. (1986)

3.5 Reduction potential at different pH values

The results show that *Ws* cytochrome c_{552} has a quasi-reversible electrochemical behavior, as expected considering similar protein systems (Santos et al., 2015; Teixeira et al., 2019). The cyclic voltammogram at pH 7.0 shows a redox process, with broad anodic and cathodic peaks (Figure 5A). The formal reduction potential calculated from the average of E_{pa} and E_{pc} is +97 ± 5 mV vs. NHE. This experimentally estimated formal reduction potential is in agreement with the previously reported value for this protein of +105 ± 15 mV, obtained by potentiometry (Moura et al., 1988). The relative difference can be explained by the different techniques used.

The study of the redox behavior at different pH values, shows that at pH values lower than pH 7.0, the potential waves are relatively better defined, and a single redox process is observed (Supplementary Figure S8, in the Supplementary Material). Above pH 7.0, a broadening of the waves (both cathodic and anodic) occurs, but it is not possible to distinguish the processes. This behavior, if only pH 7.0 was considered, could be related to some dispersion of the heterogeneous electron transfer rate constants, due to multiple electron transfer pathways. However, the global redox behavior at different pH values points to the coexistence of two slightly different protein forms regarding the heme environment, which is consistent with the hypothesis of having an oxygenated species (OH^-) or a water molecule binding/leaving at the distal axial position. The pH dependence of the redox potential considering only one acid/base group model is fitted with a pK_a values for the oxidized and reduced states: pK_{ox} and a pK_{red} of 6.9 and 7.3, respectively, with a calculated theoretical reduction potential of 0.122 V (pH 0) (Figure 5B).

4 Discussion

4.1 Structure and redox properties

W. succinogenes cytochrome c_{552} is an 81-residue *c*-type cytochrome that has been successfully heterologously

produced in *E. coli*. It is an interesting protein because it is one of the shortest *c*-type cytochromes isolated to date and has unusual spectroscopic and redox properties, namely, a low reduction potential (+97 mV, pH 7.0) and the coexistence of a high and a low spin form at room temperature. Other small cytochromes have a similar reduction potential, but the high/low spin coexistence has not been reported (Table 2). Comparing its model structure, presented here, for the first time, it is clear that due to the shorter polypeptide chain, the heme is more exposed to the solvent, and not in the usual hydrophobic environment with only the exposed heme edge to the solvent (Figure 1) as in the case of *P. denitrificans* cytochrome c_{550}. This solvent exposure may explain its lower reduction potential. Indeed, cytochrome c_{553} from *N. vulgaris Hildenborough* also has a low reduction potential, which has been attributed to the greater exposure of the heme to the solvent (Blackledge et al., 1996). An exception is the cytochrome c_{552} from *M. nauticus*, which has a much higher reduction potential despite being 88 residues long and having a similar structure (Table 2). However, this cytochrome c_{552} is a dimer in which the propionate groups are shielded from the solvent because they are located at the dimer interface (Supplementary Figure S11, in the Supplementary Material).

4.2 Effect of pH

The effect of pH on the redox properties of *W. succinogenes* cytochrome c_{552} differs from that reported for *N. vulgaris* cytochrome c_{553}, both in the shape of the cyclic voltammograms and in the estimated p*K*a. Similar to other class I *c*-type cytochromes, *N. vulgaris* cytochrome c_{553} shows no effect on the reduction potential up to pH 10.0 (Verhagen et al., 1994), after which there is a marked decrease in the reduction potential, which has been attributed to the loss of the methionine as a distal axial ligand with a pK_a of 10.9 (Verhagen et al., 1994). The pH dependence of *Ws* cytochrome c_{552} was studied only up to pH 9.0 to avoid its destabilization close to its pI (of 8.6) and shows a close pK_{ox}/pK_{red}, of 6.9/7.3, a lower value. Furthermore, the voltammograms indicate the presence of two forms, with similar reduction potential. Curiously, *M. nauticus* cytochrome c_{552} has a similar pKa observed in the redox potential determined by potentiometry (Saraiva et al., 1994), but not by cyclic voltammetry (data not shown) (Coutinho, 2013).

The observed band at 620 nm decreases in intensity with the increasing of the pH, while the band at 695 nm (due to the axially coordinated methionine) increases in intensity. This can be explained by the fact that the methionine ligand becomes strongly bound to the heme iron, and thus the heme becomes low spin, while at low pHs the methionine can be partially replaced by a low-field ligand, possibly OH^-, which can be protonated to water. This could explain the observed low-spin EPR signal (Moura et al., 1988), since it can have a temperature-dependent high/low-spin equilibrium (Barreiro et al., 2023a). Another possible explanation for the observed equilibrium could be the protonation/deprotonation of the propionates. In any case both hypotheses do not promote structural changes in the heme pocket, since the near-UV/visible CD spectra do not change with pH (Supplementary Figure S6, in the Supplementary Material).

4.3 Thermostability

The thermostability of *W. succinogenes* cytochrome c_{552} has been studied for the first time by CD and DSC. The T_M values estimated by the two complementary techniques are similar, but no other thermodynamic parameters can be estimated because the unfolding process is irreversible. This *c*-type cytochrome is rather stable, and its stability decreases close to its pI. The effect of pH on the thermostability of some *c*-type cytochromes has been studied at very low pH values (Kuroda et al., 1992). However, there are no reports on the effect of pH on the thermostability of *c*-type cytochromes in the range studied here, so the destabilization at high pH, observed for *Ws* cytochrome c_{552}, may be due to a change in the hydrogen bonds that stabilize the structure of this protein.

The unfolding temperature observed at pH 7.0 is relatively higher than that observed for other proteins isolated from mesophilic bacteria (Nobrega et al., 2017), although some exceptions have been reported (Barreiro et al., 2023b). However, the T_M is relatively low (90°C, at pH 5.0) compared to that of cytochrome c_{552} from thermophilic organisms: *Hydrogenophilus thermoluteolus* and *H. thermophilus*, which have a T_M of 108°C and 121°C, respectively, at pH 5.0 (Oikawa et al., 2005; Nakamura et al., 2006). These two *c*-type cytochromes are as small as *Ws* cytochrome c_{552}, containing about 80 residues. Interestingly, however, although composed of only 4 α-helices, there is a loop protecting the 6-propionate group of the porphyrin ring (Supplementary Figure S12, in the Supplementary Material), which is absent in *W. succinogenes* cytochrome c_{552}.

Furthermore, *Pseudomonas aeruginosa* cytochrome c_{551}, being an 82-residue protein from a mesophilic organism, has a T_M of 85°C, at pH 7.0 (Sanbongi et al., 1989), which compares well with the unfolding temperature of *W. succinogenes* cytochrome c_{552}, at pH 7.0 (80°C). The structure of this cytochrome c_{551} is similar to the previously mentioned highly thermostable *c*-type cytochromes, with the 4 α-helices and the loop protecting the 6-propionate, so perhaps the exposed heme does not affect the thermostability of the protein as much. In fact, some residues have been proposed to be the main cause of thermostability between *H. thermophilus* cytochrome c_{552} and *P. aeruginosa* cytochrome c_{551} (Oikawa et al., 2005), suggesting that the stabilization may be due to side-chain interactions.

Data availability statement

The original contributions presented in the study are included in the article/Supplementary Material, further inquiries can be directed to the corresponding author.

Author contributions

VM: Investigation, Writing–review and editing. MC: Formal Analysis, Investigation, Methodology, Supervision, Writing–review and editing. CC: Formal Analysis, Investigation, Writing–review and editing. NP: Writing–review and editing, Investigation. JS: Writing–review and editing. IM: Funding acquisition, Writing–review and editing. SP: Conceptualization, Data curation, Formal Analysis, Investigation, Methodology, Supervision, Visualization, Writing–original draft, Writing–review and editing.

Funding

The author(s) declare that financial support was received for the research, authorship, and/or publication of this article. This research was funded by Fundação para a Ciência e a Tecnologia, I.P. (FCT), through a project grant to IM(2022.01152. PTDC). This work was also supported by national funds from FCT in the scope of the project UIDP/04378/2020 and UIDB/04378/2020 of the Research Unit on Applied Molecular Biosciences-UCIBIO and the project LA/P/0140/2020 of the Associate Laboratory Institute for Health and Bioeconomy-i4HB, and projects 10.54499/UIDB/50006/2020, 10.54499/UIDP/50006/2020, and 10.54499/LA/P/0008/2020 of the Associated Laboratory for Green Chemistry (LAQV).

Acknowledgments

The authors acknowledge the Biolab for the acquisition of CD and DSC data, and Hugo Santos and the BIOSCOPE group for determining the molecular mass by LC-ESI-MS of the isolated *Ws* cytochrome c_{552}.

Conflict of interest

The authors declare that the research was conducted in the absence of any commercial or financial relationships that could be construed as a potential conflict of interest.

Publisher's note

All claims expressed in this article are solely those of the authors and do not necessarily represent those of their affiliated organizations, or those of the publisher, the editors and the reviewers. Any product that may be evaluated in this article, or claim that may be made by its manufacturer, is not guaranteed or endorsed by the publisher.

Supplementary material

The Supplementary Material for this article can be found online at: https://www.frontiersin.org/articles/10.3389/fchbi.2024.1398105/full#supplementary-material

References

Anthis, N. J., and Clore, G. M. (2013). Sequence-specific determination of protein and peptide concentrations by absorbance at 205 nm. *Protein Sci.* 22 (6), 851–858. doi:10.1002/pro.2253

Arslan, E., Schulz, H., Zufferey, R., Kunzler, P., and Thony-Meyer, L. (1998). Overproduction of the *Bradyrhizobium japonicum c*-type cytochrome subunits of the cbb_3 oxidase in *Escherichia coli*. *Biochem. Biophysical Res. Commun.* 251 (3), 744–747. doi:10.1006/bbrc.1998.9549

Baar, C., Eppinger, M., Raddatz, G., Simon, J., Lanz, C., Klimmek, O., et al. (2003). Complete genome sequence and analysis of *Wolinella succinogenes*. *Proc. Natl. Acad. Sci. U. S. A.* 100 (20), 11690–11695. doi:10.1073/pnas.1932838100

Barreiro, D. S., Oliveira, R. N. S., and Pauleta, S. R. (2023a). Bacterial peroxidases – multivalent enzymes that enable the use of hydrogen peroxide for microaerobic and anaerobic proliferation. *Coord. Chem. Rev.* 485, 215114. doi:10.1016/j.ccr.2023.215114

Barreiro, D. S., Oliveira, R. N. S., and Pauleta, S. R. (2023b). Biochemical characterization of the copper nitrite reductase from *Neisseria gonorrhoeae*. *Biomolecules* 13 (8), 1215. doi:10.3390/biom13081215

Berry, E. A., and Trumpower, B. L. (1987). Simultaneous determination of hemes *a*, *b*, and *c* from pyridine hemochrome spectra. *Anal. Biochem.* 161 (1), 1–15. doi:10.1016/0003-2697(87)90643-9

Bertini, I., Cavallaro, G., and Rosato, A. (2006). Cytochrome *c*: occurrence and functions. *Chem. Rev.* 106 (1), 90–115. doi:10.1021/cr050241v

Besson, S., Almeida, M. G., and Silveira, C. M. (2022). Nitrite reduction in bacteria: a comprehensive view of nitrite reductases. *Coord. Chem. Rev.* 464, 214560. doi:10.1016/j.ccr.2022.214560

Blackledge, M. J., Guerlesquin, F., and Marion, D. (1996). Comparison of low oxidoreduction potential cytochrome c553 from Desulfovibrio vulgaris with the class I cytochrome c family. *Proteins* 24 (2), 178–194. doi:10.1002/(SICI)1097-0134(199602)24:2<178::AID-PROT5>3.0.CO;2-F

Coutinho, I. C. R. F. (2013) A peroxidase do citocromo c de Marinobacter hydrocarbonoclasticus 617: aplicação de técnicas espectroscópicas e electroquímicas ao estudo do mecanismo de activação e catálise. PhD thesis. Lisbon, Portugal: Universidade Nova de Lisboa.

Dell'acqua, S., Moura, I., Moura, J. J., and Pauleta, S. R. (2011). The electron transfer complex between nitrous oxide reductase and its electron donors. *J. Biol. Inorg. Chem.* 16 (8), 1241–1254. doi:10.1007/s00775-011-0812-9

Dell'Acqua, S., Pauleta, S. R., Monzani, E., Pereira, A. S., Casella, L., Moura, J. J. G., et al. (2008). Electron transfer complex between nitrous oxide reductase and cytochrome c_{552} from *Pseudomonas nautica*: kinetic, nuclear magnetic resonance, and docking studies. *Biochemistry* 47 (41), 10852–10862. doi:10.1021/bi801375q

Ferri, T., Poscia, A., Ascoli, F., and Santucci, R. (1996). Direct electrochemical evidence for an equilibrium intermediate in the guanidine-induced unfolding of cytochrome *c*. *Biochimica Biophysica Acta (BBA) - Protein Struct. Mol. Enzym.* 1298 (1), 102–108. doi:10.1016/S0167-4838(96)00122-7

Fujita, K., Hirasawa-Fujita, M., Brown, D. E., Obara, Y., Ijima, F., Kohzuma, T., et al. (2012). Direct electron transfer from pseudoazurin to nitrous oxide reductase in catalytic N_2O reduction. *J. Inorg. Biochem.* 115, 163–173. doi:10.1016/j.jinorgbio.2012.07.013

Goodhew, C. F., Brown, K. R., and Pettigrew, G. W. (1986). Haem staining in gels, a useful tool in the study of bacterial *c*-type cytochromes. *Biochimica Biophysica Acta (BBA) - Bioenergetics* 852 (2-3), 288–294. doi:10.1016/0005-2728(86)90234-3

Gray, K. A., Knaff, D. B., Husain, M., and Davidson, V. L. (1986). Measurement of the oxidation-reduction potentials of amicyanin and *c*-type cytochromes from *Paracoccus denitrificans*. *FEBS Lett.* 207 (2), 239–242. doi:10.1016/0014-5793(86)81496-x

Greenfield, N. J. (2004). Analysis of circular dichroism data. *Methods Enzym.* 383, 282–317. doi:10.1016/S0076-6879(04)83012-X

Hon-nami, K., and Oshima, T. (1977). Purification and some properties of cytochrome c_{-552} from an extreme thermophile, *Thermus thermophilus* HB8. *J. Biochem.* 82 (3), 769–776. doi:10.1093/oxfordjournals.jbchem.a131753

Jumper, J., Evans, R., Pritzel, A., Green, T., Figurnov, M., Ronneberger, O., et al. (2021). Highly accurate protein structure prediction with AlphaFold. *Nature* 596 (7873), 583–589. doi:10.1038/s41586-021-03819-2

Kern, M., Eisel, F., Scheithauer, J., Kranz, R. G., and Simon, J. (2010). Substrate specificity of three cytochrome *c* haem lyase isoenzymes from *Wolinella succinogenes*: unconventional haem *c* binding motifs are not sufficient for haem *c* attachment by NrfI and CcsA1. *Mol. Microbiol.* 75 (1), 122–137. doi:10.1111/j.1365-2958.2009.06965.x

Kern, M., and Simon, J. (2009). Electron transport chains and bioenergetics of respiratory nitrogen metabolism in *Wolinella succinogenes* and other Epsilonproteobacteria. *Biochimica Biophysica Acta (BBA) - Bioenergetics* 1787 (6), 646–656. doi:10.1016/j.bbabio.2008.12.010

Kuroda, Y., Kidokoro, S.-i., and Wada, A. (1992). Thermodynamic characterization of cytochrome *c* at low pH: observation of the molten globule state and of the cold denaturation process. *J. Mol. Biol.* 223 (4), 1139–1153. doi:10.1016/0022-2836(92)90265-L

Micsonai, A., Bulyáki, É., and Kardos, J. (2021). "BeStSel: from secondary structure analysis to protein fold prediction by circular dichroism spectroscopy," in *Structural genomics: general applications*. Editors Y. W. Chen and C.-P. B. Yiu (New York, NY: Springer US), 175–189.

Micsonai, A., Moussong, É., Wien, F., Boros, E., Vadászi, H., Murvai, N., et al. (2022). BeStSel: webserver for secondary structure and fold prediction for protein CD spectroscopy. *Nucleic Acids Res.* 50 (W1), W90–W98. doi:10.1093/nar/gkac345

Moura, I., Liu, M. Y., Costa, C., Liu, M. C., Pai, G., Xavier, A. V., et al. (1988). Spectroscopic characterization of a high-potential monohaem cytochrome from *Wolinella succinogenes*, a nitrate-respiring organism. *Eur. J. Biochem.* 177 (3), 673–682. doi:10.1111/j.1432-1033.1988.tb14421.x

Nagai, M., Kobayashi, C., Nagai, Y., Imai, K., Mizusawa, N., Sakurai, H., et al. (2015). Involvement of propionate side chains of the heme in circular dichroism of myoglobin: experimental and theoretical analyses. *J. Phys. Chem. B* 119 (4), 1275–1287. doi:10.1021/jp5086203

Nakamura, S., Ichiki, S.-i., Takashima, H., Uchiyama, S., Hasegawa, J., Kobayashi, Y., et al. (2006). Structure of cytochrome c_{552} from a moderate thermophilic bacterium, *Hydrogenophilus thermoluteolus*: comparative study on the thermostability of cytochrome *c*. *Biochemistry* 45 (19), 6115–6123. doi:10.1021/bi0520131

Nobrega, C. S., Raposo, M., Van Driessche, G., Devreese, B., and Pauleta, S. R. (2017). Biochemical characterization of the bacterial peroxidase from the human pathogen *Neisseria gonorrhoeae*. *J. Inorg. Biochem.* 171, 108–119. doi:10.1016/j.jinorgbio.2017.03.007

Oikawa, K., Nakamura, S., Sonoyama, T., Ohshima, A., Kobayashi, Y., Takayama, S.-i.J., et al. (2005). Five amino acid residues responsible for the high stability of *Hydrogenobacter thermophilus* cytochrome c_{552}: reciprocal mutation analysis. *J. Biol. Chem.* 280 (7), 5527–5532. doi:10.1074/jbc.M412392200

Pauleta, S. R., Carepo, M. S. P., and Moura, I. (2019). Source and reduction of nitrous oxide. *Coord. Chem. Rev.* 387, 436–449. doi:10.1016/j.ccr.2019.02.005

Pauleta, S. R., Dell'Acqua, S., and Moura, I. (2013). Nitrous oxide reductase. *Coord. Chem. Rev.* 257 (2), 332–349. doi:10.1016/j.ccr.2012.05.026

Payne, W. J., Grant, M. A., Shapleigh, J., and Hoffman, P. (1982). Nitrogen oxide reduction in *Wolinella succinogenes* and *Campylobacter* species. *J. Bacteriol.* 152 (2), 915–918. doi:10.1128/jb.152.2.915-918.1982

Pearson, I. V., Page, M. D., van Spanning, R. J., and Ferguson, S. J. (2003). A mutant of Paracoccus denitrificans with disrupted genes coding for cytochrome c550 and pseudoazurin establishes these two proteins as the *in vivo* electron donors to cytochrome cd1 nitrite reductase. *J. Bacteriol.* 185 (21), 6308–6315. doi:10.1128/JB.185.21.6308-6315.2003

Pettigrew, G. W., and Moore, G. R. (1987) *Cytochromes c*. Springer.

Pielak, G. J., Oikawa, K., Mauk, A. G., Smith, M., and Kay, C. M. (1986). Elimination of the negative soret Cotton effect of cytochrome *c* by replacement of the invariant phenylalanine using site-directed mutagenesis. *J. Am. Chem. Soc.* 108 (10), 2724–2727. doi:10.1021/ja00270a035

Samyn, B., Fitch, J., Meyer, T. E., Cusanovich, M. A., and Van Beeumen, J. J. (1998). Purification and primary structure analysis of two cytochrome c_2 isozymes from the purple phototrophic bacterium *Rhodospirillum centenum*. *Biochimica Biophysica Acta (BBA) - Protein Struct. Mol. Enzym.* 1384 (2), 345–355. doi:10.1016/s0167-4838(98)00030-2

Sanbongi, Y., Igarashi, Y., and Kodama, T. (1989). Thermostability of cytochrome c-$_{552}$ from the thermophilic hydrogen-oxidizing bacterium *Hydrogenobacter thermophilus*. *Biochemistry* 28 (25), 9574–9578. doi:10.1021/bi00451a004

Santos, T. C., de Oliveira, A. R., Dantas, J. M., Salgueiro, C. A., and Cordas, C. M. (2015). Thermodynamic and kinetic characterization of PccH, a key protein in microbial electrosynthesis processes in *Geobacter sulfurreducens*. *Biochimica Biophysica Acta (BBA) - Bioenergetics* 1847 (10), 1113–1118. doi:10.1016/j.bbabio.2015.06.005

Saraiva, L. M., Fauque, G., Besson, S., and Moura, I. (1994). Physico-chemical and spectroscopic properties of the monohemic cytochrome c_{552} from *Pseudomonas nautica* 617. *Eur. J. Biochem.* 224 (3), 1011–1017. doi:10.1111/j.1432-1033.1994.01011.x

Senn, H., and Wüthrich, K. (1985). Amino acid sequence, haem-iron co-ordination geometry and functional properties of mitochondrial and bacterial *c*-type cytochromes. *Q. Rev. Biophysics* 18 (2), 111–134. doi:10.1017/s0033583500005151

Shiro, Y. (2012). Structure and function of bacterial nitric oxide reductases: nitric oxide reductase, anaerobic enzymes. *Biochimica Biophysica Acta (BBA) - Bioenergetics* 1817 (10), 1907–1913. doi:10.1016/j.bbabio.2012.03.001

Sievers, F., Wilm, A., Dineen, D., Gibson, T. J., Karplus, K., Li, W., et al. (2011). Fast, scalable generation of high-quality protein multiple sequence alignments using Clustal Omega. *Mol. Syst. Biol.* 7 (1), 539. doi:10.1038/msb.2011.75

Sparacino-Watkins, C., Stolz, J. F., and Basu, P. (2014). Nitrate and periplasmic nitrate reductases. *Chem. Soc. Rev.* 43 (2), 676–706. doi:10.1039/C3CS60249D

Teixeira, L. R., Cordas, C. M., Fonseca, M. P., Duke, N. E. C., Pokkuluri, P. R., and Salgueiro, C. A. (2019). Modulation of the redox potential and electron/proton transfer mechanisms in the outer membrane cytochrome OmcF from *Geobacter sulfurreducens*. *Front. Microbiol.* 10, 2941. doi:10.3389/fmicb.2019.02941

Teraguchi, S., and Hollocher, T. C. (1989). Purification and some characteristics of a cytochrome *c*-containing nitrous oxide reductase from *Wolinella succinogenes*. *J. Biol. Chem.* 264 (4), 1972–1979. doi:10.1016/s0021-9258(18)94130-x

Teufel, F., Almagro Armenteros, J. J., Johansen, A. R., Gíslason, M. H., Pihl, S. I., Tsirigos, K. D., et al. (2022). SignalP 6.0 predicts all five types of signal peptides using protein language models. *Nat. Biotechnol.* 40 (7), 1023–1025. doi:10.1038/s41587-021-01156-3

Verhagen, M. F., Wolbert, R. B., and Hagen, W. R. (1994). Cytochrome c_{553} from *Desulfovibrio vulgaris* (Hildenborough). Electrochemical properties and electron transfer with hydrogenase. *Eur. J. Biochem.* 221 (2), 821–829. doi:10.1111/j.1432-1033.1994.tb18796.x

Vinogradov, S., and Zand, R. (1968). Circular dichroism studies: I. Cytochrome *c*. *Archives Biochem. Biophysics* 125 (3), 902–910. doi:10.1016/0003-9861(68)90529-8

Wittung-Stafshede, P. (1999). Equilibrium unfolding of a small low-potential cytochrome, cytochrome c_{553} from *Desulfovibrio vulgaris*. *Protein Sci.* 8 (7), 1523–1529. doi:10.1110/ps.8.7.1523

Woody, R. W., and Hsu, M. C. (1971). Origin of the heme Cotton effects in myoglobin and hemoglobin. *J. Am. Chem. Soc.* 93 (14), 3515–3525. doi:10.1021/ja00743a036

Zhang, C.-s., and Hollocher, T. C. (1993). The reaction of reduced cytochromes *c* with nitrous oxide reductase of *Wolinella succinogenes*. *Biochimica Biophysica Acta (BBA) - Bioenergetics* 1142 (3), 253–261. doi:10.1016/0005-2728(93)90153-7